Inhibitor-Resistant Class A β-Lactamases: Consequences of the Ser130-to-Gly Mutation Seen in Apo and Tazobactam Structures of the SHV-1 Variant[†,‡]

Tao Sun,[§] Christopher R. Bethel,[||] Robert A. Bonomo,[||] and James R. Knox*[,§]

Department of Molecular and Cell Biology, The University of Connecticut, Storrs, Connecticut 06269-3125, and Research Service, Department of Veterans Affairs Medical Center, Cleveland, Ohio 44106

Received June 10, 2004; Revised Manuscript Received August 27, 2004

ABSTRACT: A bacterial response to the clinical use of class A β-lactamase inhibitors such as tazobactam and clavulanic acid is the expression of variant β-lactamases with weaker binding affinities for these mechanism-based inhibitors. Some of these inhibitor-resistant variants contain a glycine mutation at Ser130, a conserved active site residue known to be adventitiously involved in the inhibition mechanism. The crystallographic structure of a complex of tazobactam with the Ser130Gly variant of the class A SHV-1 β-lactamase has been determined to 1.8 Å resolution. Two reaction intermediates are observed. The primary intermediate is an acyclic species bound to the reactive Ser70. It is poorly primed for catalytic hydrolysis because its ester carbonyl group is completely displaced from the enzyme's oxyanion hole. A smaller fraction of the enzyme contains a Ser70-bound aldehyde resulting from hydrolytic loss of the triazoyl−sulfinyl amino acid moiety from the primary species. This first structure of a class A β-lactamase lacking Ser130, the side chain of which functions in β-lactam binding and possibly in catalysis, gives crystallographic evidence that the acylation step of β-lactam turnover can occur without Ser130. Unexpectedly, the crystal structure of the uncomplexed Ser130Gly enzyme, also determined to 1.8 Å resolution, shows that a critical Glu166-activated water molecule is missing from the catalytic site. Comparison of this uncomplexed variant with the wild-type structure reveals that Ser130 is required for orienting the side chain of Ser70 and ensuring the hydrogen bonding of Ser70 to both Lys73 and the catalytic water molecule.

Inhibition of bacterial β-lactamases has been sought for nearly half a century (*1*−*3*). These troublesome enzymes hydrolyze β-lactam antibiotics (penicillins, cephalosporins, and carbapenems) with catalytic efficiencies of up to 10^6 mM^{-1} s^{-1} (*4*). Either chromosomal or plasmid-borne, these hydrolases have been placed into four sequence-based classes (A−D) and further divided into subgroups according to their reactivity with β-lactams and inhibitors (*5*). Natural variants with expanded β-lactam profiles continue to appear in clinical environments and now number in the hundreds (*6*; see //www.lahey.org/studies/webt.asp). Some of the class A variants possess an alarming resistance to valuable mechanism-based inhibitors such as tazobactam (**1**), sulbactam, and clavulanic acid (*7*, *8*).

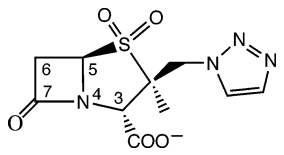

1

In the homologous SHV and TEM β-lactamase families, these inhibitor-resistant enzymes generally contain a mutation at position Met69, Ser130, Arg244, or Asn276, and as a result, they often exhibit impaired catalytic efficiency for the hydrolysis of β-lactam substrates (*9*−*12*). For example, the conserved Ser130 is thought to be important for maintaining thermal stability (*13*), hydrogen bonding with the C3 carboxylic acid group of β-lactam substrates, especially cephalosporins (*14*), and possibly for aiding catalysis by assisting transfer of protons to and from the reactive Ser70 (*15*, *16*).

Crystallographic (*17*) and mass spectrometry studies (*18*−*20*) of the reaction of SHV-type and TEM-type β-lactamases with tazobactam and clavulanic acid showed that Ser130, as well as the catalytic Ser70, is covalently modified in the inhibition process, a chemistry predicted earlier by a molecular dynamics simulation (*21*). The experimental studies found that nucleophilic attack by the Ser130 hydroxyl group on a Ser70-bound acyclic intermediate produced a more stable Ser130-bound acrylic acid fragment capable of preventing entry of the β-lactam substrate into the catalytic site, and thus providing irreversible inhibition (Figure 1). To understand how natural mutants lacking Ser130 exhibit a transient inhibition, we have established the crystallographic structure of the reaction product of tazobactam with the Ser130Gly SHV-1 variant, known to have a lowered affinity and a reduced k_{cat} for the tazobactam and clavulanic acid inhibitors (*12*). In addition, we report a significant and perplexing change in the hydration of the catalytic site of the uncomplexed (apo) Ser130Gly structure relative to the WT[1] SHV-1 structure (*22*).

[†] Work was supported in part by a Merit Review Grant from the Veterans Administration to R.A.B. and by NIH Grant AI-52216 to J.R.K.

[‡] Atomic coordinates and structure factors have been deposited in the Protein Data Bank at the Research Collaboratory for Structural Bioinformatics at Rutgers University (entries 1TDG and 1TDL for the complexed and apo structures, respectively).

* To whom correspondence should be addressed. Phone: (860) 486-3133. Fax: (860) 486-4745. E-mail: james.knox@uconn.edu.

[§] The University of Connecticut.

[||] Veterans Affairs Medical Center.

10.1021/bi0487903 CCC: $27.50
Published on Web 10/16/2004

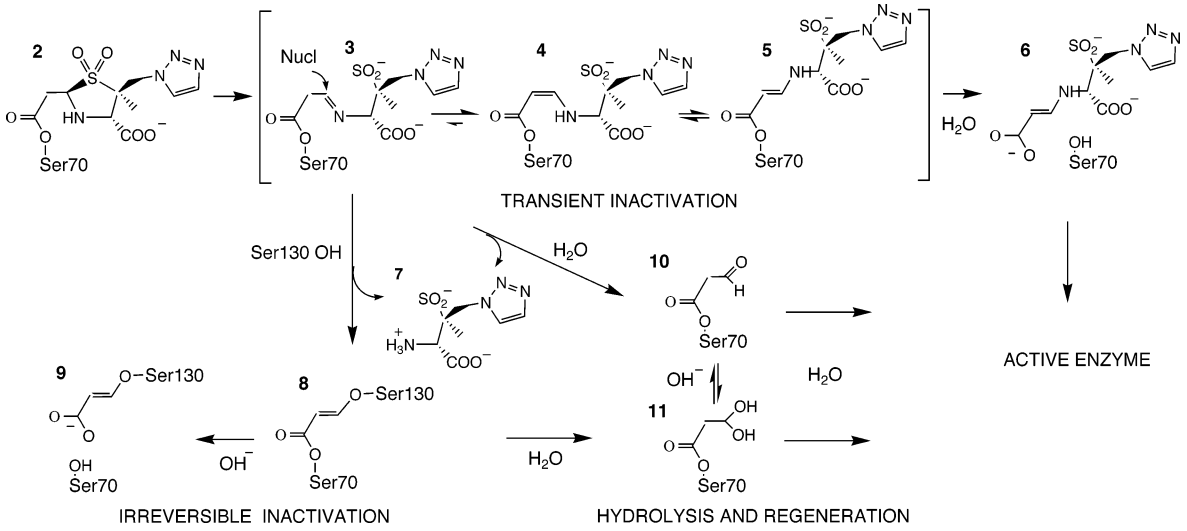

FIGURE 1: Proposed reaction of tazobactam with class A β-lactamases (*17*).

MATERIALS AND METHODS

Protein Production. PCR-based site saturation and site-directed mutagenesis were performed using Stratagene's QuikChange Mutagenesis Kit as previously reported to create the Ser130Gly substituted SHV-1 β-lactamase (*12*, *23*). The enzyme was purified to homogeneity from *Escherichia coli* DH10B cells according to a method employing preparative isoelectric focusing (*12*). The purity was assessed on 5% stacking, 12% resolving SDS−PAGE gels stained with Coomassie Brilliant Blue R250 (Fisher, Pittsburgh, PA). Protein concentrations were determined with the Bio-Rad (Hercules, CA) Protein Assay using bovine serum albumin as a standard.

Crystallization of the Variant β-Lactamase. The sitting-drop vapor diffusion method was applied for Ser130Gly SHV-1 crystallization at room temperature. A 10 μL crystallization drop (containing 3 μL of 5 mg/mL protein, 1 μL of 5.6 mM Cymal-6 detergent, and 6 μL of reservoir) was placed over a 0.75 mL reservoir [30% PEG 6000 and 0.1 M HEPES (pH 7.0)]. Cubic-shaped crystals grew to 0.15 mm in each dimension in 1 month.

Reaction with the Inhibitor. Tazobactam (99.5%) was a gift of Wyeth Pharmaceuticals (Pearl River, NY). A pregrown crystal of Ser130Gly SHV-1 was soaked at 21 °C for 3 h in a 30% PEG holding solution [HEPES (pH 7)] containing 20 mM tazobactam. A half-volume of the soaking solution was refreshed every 30 min.

X-ray Data Collection. Diffraction data were collected with a Rigaku RU-200 rotating anode generator operating at 40 kV and 60 mA ($\lambda = 1.542$ Å), and with double-mirror Franks focusing, a Bruker HISTAR multiwire area detector, and an Oxford Cryosystems nitrogen gas stream at 100 K. For cryoprotection, 25% MPD was added to the holding solution, in which the crystal was soaked for ~1 min before being placed in the X-ray beam. At a detector distance of 10 cm, the ω angle was swept for 180° in 0.2° steps. Two sweeps at 32° (2θ) with 120 s per frame were followed by one sweep at 0° with 10 s per frame. XGEN (Molecular Simulations, Inc.) reduced, scaled, and integrated the raw intensities, and showed that the data reached to 1.66 Å. Because the completeness of the highest shell was less than 50%, the data used for final structure refinement were truncated at 1.80 Å. The space group is $P2_12_12_1$ with one 28.9 kDa molecule per asymmetric unit, similar to the WT SHV-1 crystals (*22*). The Matthews coefficient is 1.99 Å^3/Da, and the solvent content is 38%. Data are given in Table 1.

Table 1: X-ray Data Collection (100 K) for Ser130Gly SHV-1[a]

	complexed	uncomplexed
resolution range (Å)	20−1.80	20−1.80
cell dimensions [*a*, *b*, *c* (Å)]	49.8, 55.3, 83.6	49.6, 55.3, 84.1
no. of observations	123653 (9409)	102682 (10729)
no. of unique reflections	20318 (2868)	20676 (3079)
completeness	0.922 (0.791)	0.936 (0.846)
average $I/\sigma(I)$	14.8 (4.5)	34.6 (12.1)
$R_{sym}(I)$[b]	0.059 (0.138)	0.033 (0.068)

[a] Data for the 1.91−1.80 Å shell are in parentheses. [b] $R_{sym} = \sum|I_{av} - I_i|/\sum I_i$, where I_{av} is the average of all individual observations, I_i. The space group is $P2_12_12_1$.

RESULTS

Structure Determination. The uncomplexed WT SHV-1 β-lactamase (PDB entry 1SHV) was used as the search model in molecular replacement calculations. EPMR (*24*) using data in the resolution range of 15−4 Å found a solution with correlation coefficient of 0.75 and an R of 0.325. Rigid-body refinement with data from 6 to 1.7 Å improved the match ($R = 0.305$ and $R_{free} = 0.332$).

Structure Refinement. All of the reflections for which $|F| > 0\sigma(F)$ were used for the refinement, 5% of which were selected randomly for the R_{free} calculation. CNS (*25*) was employed using a bulk solvent correction, anisotropic initial B-factor correction, and a maximum likelihood target. Composite omit maps displayed with CHAIN (*26*) were used for manual fitting and to minimize model bias. In the initial refinement cycles, simulated annealing with starting temperatures from 2000 to 300 K was used. After refinement reached $R = 0.25$ ($R_{free} = 0.32$) at 2.5 Å, water molecules and a Cymal-6 detergent molecule were added to the model. Further inclusion of group and atom B-factor refinements, alternate side chain conformations, part of a second Cymal-6

[1] Abbreviations: Cymal-6, cyclohexyl(*n*-hexyl)-β-D-maltoside; HEPES, *N*-(2-hydroxyethyl)piperazine-*N*′-2-ethanesulfonic acid; MPD, 2-methyl-2,4-pentanediol; PEG, poly(ethylene glycol); rmsd, root-mean-square deviation; WT, wild-type.

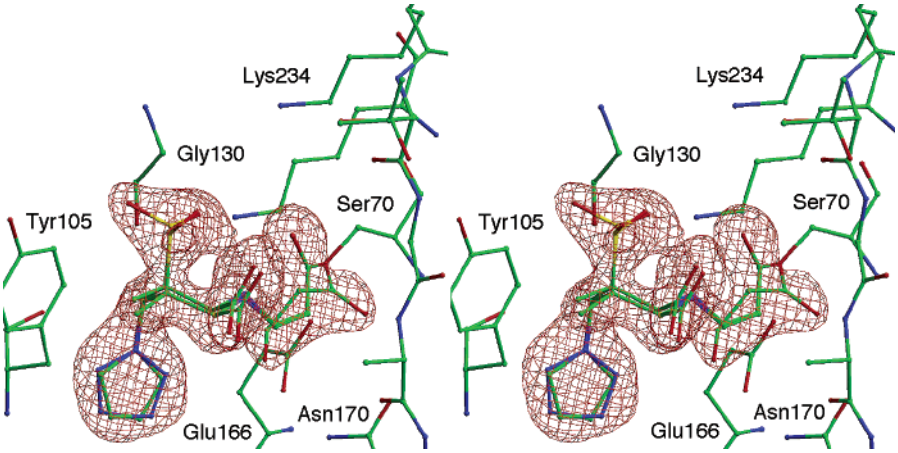

FIGURE 2: Stereoview of the $F_o - F_c$ electron density of the intermediates bonded to the reactive Ser70 in the Ser130Gly SHV-1 β-lactamase. The contour level is 3.0σ. This figure was created with XtalView (*33*) and Raster3D (*34*).

Table 2: Dihedral Angles (deg) in Three Tazobactam Intermediates

	3−**4** in Ser130Gly[a]	**10** in Ser130Gly	**3** in WT[b]
Ser70 N−Cα−Cβ−Oγ	−69	−69	−70
Cα−Cβ−Oγ−C7	151	104	96
Cβ−Oγ−C7−C6	−127	110	176
Oγ−C7−C6−C5	−155	97	168
C7−C6−C5−N4	0	120	113
C6−C5−N4−C3	−177	−	144
C5−N4−C3−C2	−151	−	−116
N4−C3−C2−S1	−58	−	−2

[a] Average of two rotamers. [b] From ref *17*.

Table 3: Crystallographic Refinement for Ser130Gly SHV-1

	complexed	uncomplexed
resolution range (Å)	20−1.80 (1.91−1.80)	20−1.80 (1.91−1.80)
no. of reflections used [$F > 0\sigma(F)$]	20094 (2769)	20611 (3041)
R-factor	0.140 (0.175)	0.142 (0.167)
R_{free} from 5% of the data	0.176 (0.204)	0.181 (0.242)
residues in Ramachandran zones (%)		
most favored	92.2	91.3
additional allowed	7.8	8.3
generously allowed	0	0.4
rms deviations from ideality		
bond lengths (Å)	0.007	0.007
bond angles (deg)	1.4	1.4
dihedrals (deg)	24.5	21.9
impropers (deg)	0.8	1.4
mean *B*-factors [Å^2 (no. of atoms)]		
protein atoms	7.5 (2022)	7.9 (2022)
tazobactam species	14.2 (25)	−
water molecules	29.5 (396)	29.5 (414)
Cymal-6 detergent	10.9 (45)	14.1 (45)
MPD, HEPES	23.7 (16), −	−, 47.5 (5)
all atoms	10.9 (2504)	11.4 (2486)

molecule, and two MPD molecules gave an *R* of 0.18 (R_{free} = 0.22) at 1.8 Å. At this stage, electron density emanating from Ser70 at the 3σ level was clear and continuous. Especially prominent was a flat density peak that identified the triazoyl ring of tazobactam.

Modeling the Intermediates. Crystallographic discrimination between single and double bonds in the reaction products of Figure 1 was not certain at this resolution. Dihedral angles were useful indicators, however (Table 2). All atoms of the C3−N4−C5−C6−C7 fragment were nearly coplanar with a trans dihedral angle around the N4−C5 bond (−175°). Of two possible C5−C6 tautomers, **4** and **5**, only the cis enamine **4** could be fit to the difference density. Favorable hydrogen bond geometry between N4 and an oxygen atom in the SO_2 group (2.8 Å) further suggested a contribution from species **4**. Nevertheless, the imine **3** could not be ruled out and is probably in equilibrium with enamine **4**. Residual density and patterns of hydrogen bonding to water indicated that the **3**−**4** intermediate contained an alternate rotamer of the SO_2 and triazoyl groups. Even in early maps it was notable that the ester carbonyl group was not bound in the oxyanion hole formed by the backbone amides of Ser70 and Ala237. A similar out-of-hole acyl intermediate was found in two complexes of the class A TEM-1 β-lactamase (*27*, *28*) and in a class C complex (*29*). A substrate omit map showed weak residual density in the oxyanion hole and also protruding near C5. Assuming a mixture of two intermediates exists in the crystal, the hydrolysis product aldehyde **10**, with its ester carbonyl oxygen atom in the oxyanion hole, was added over the major **3**−**4** species (Figure 2). The decision to place the carbonyl group of the **3**−**4** species outside of the oxyanion hole, and species **10** in the hole, was based on the fact that the electron densities of the sulfinyl, carboxylic acid, and triazoyl groups were as strong as the density of the out-of-hole carbonyl group. Density for the carbonyl group in the oxyanion hole was much weaker. Species **11** was not modeled because there was no indication of its additional hydroxyl group.

After the occupancies of the two intermediates were adjusted so that *B*-factors approximately matched those of the Ser70 side chain atoms, the occupancies were found to sum near 1. The model now contained two rotameric conformers of the acyclic **3**−**4** species (0.33 occupancy each), one aldehyde species **10** (0.33 occupancy), all 265 amino acids, 396 water molecules for which $B < 60$ Å^2, two Cymal-6 detergent molecules (one partial), and two MPD molecules. One water molecule was found within 1 Å of the hydroxyl group of the missing Ser130 side chain and hydrogen bonded to the ammonium groups of Lys73 and Lys234. Alternate conformations were assigned to 22 amino acid side chains and to the ordered detergent molecule. Ramachandran analysis showed that 92% of residues are in most favored regions, and 8% are in additional allowed regions. The model refined to an *R* of 0.140 and an R_{free} of 0.176 for all 1.80 Å data (Table 3). Figure 3 shows the mixed α/β tertiary structure of the class A β-lactamase and the

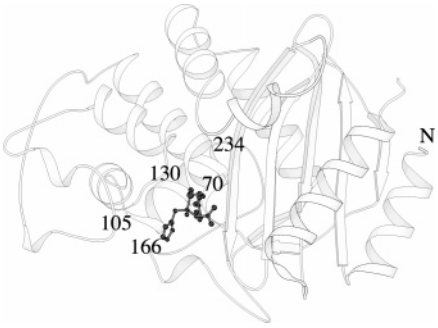

FIGURE 3: Tertiary structure of the Ser130Gly SHV-1 β-lactamase complex. Only the acyclic **3**−**4** intermediate is shown bound to Ser70. The position of Gly130 is indicated. Drawn with MOLSCRIPT (*35*).

location of inhibitor binding in the catalytic site between two domains, one entirely helical and the other a five-stranded antiparallel sheet sandwiched by helices on each surface.

Interactions of the Intermediates in the Binding Site. Except for the C2 triazoyl ring, which interacts weakly with the enzyme's Tyr105 ring through $\pi-\pi$ stacking (3.5 Å), no functional groups of the primary **3**−**4** intermediate have direct interactions with side chains in the binding site. The C2 sulfinate group is surrounded by water molecules, as is the C3 carboxylic acid group, which is generally oriented toward the electropositive side chain of Arg244. The ester carbonyl group of the **3**−**4** intermediate is not bound in the enzyme's oxyanion hole. Rather, the carbonyl oxygen atom is weakly solvated with two water molecules which form a bridge to the ammonium group of Lys234. Aldehyde **10** has its ester carbonyl group in the oxyanion hole, and its terminal carbonyl group is solvated.

Comparison with WT and Glu166Ala Tazobactam Complexes. An obvious difference exhibited by the Ser70-bound acyclic tazobactam intermediate in the Ser130Gly and WT complexes (*17*) is the disposition of the intermediate's ester carbonyl group (Figure 4). The absence of the Ser130 side chain possibly allows more thermal flexibility in the long intermediate so that the carbonyl group is pulled from the oxyanion hole of the variant. In addition, a 6 Å movement of the outer end of the **3**−**4** intermediate is observed relative to WT. In both variant and WT complexes, the C3 carboxylic acid group generally lies on the right side of the binding site, where the electropositive Lys234 and Arg244 side chains are located. However, in a tazobactam complex with the Glu166Ala SHV-1 construct (*30*), the C3 carboxylic acid group of the tazobactam is found on the left side near the position of the absent carboxylic acid group of Glu166.

Table 4: Comparison of Uncomplexed SHV-1 β-Lactamases

	Ser130Gly	WT[a]
ϕ, ψ for 130 Cα (deg)	64, 24	58, 41
ϕ, ψ for 131 Cα (deg)	−66, 115	−69, 121
130 Cα−234 Cα (Å)	8.5	8.5
130 Cα−70 Cα (Å)	7.4	6.8
70 Oγ−73 Nz (Å)	3.5	2.8
70 Oγ−130 Oγ (Å)	−	3.0
130 Oγ−234 Nz (Å)	−	3.0
catalytic water molecule	absent	present
oxyanion hole water molecule	present	present

[a] From ref *22*.

Apo Structure. The 1.8 Å crystal structure of the uncomplexed (apo) Ser130Gly enzyme was determined in a similar fashion (Tables 1 and 3). The rmsd between all Cα atoms of the apo and complexed structures is 0.12 Å. In all crystal structures of class A β-lactamases, the conserved Ser130 has an unfavorable backbone conformation with a positive ϕ angle in the α_L region of the Ramachandran plot. It is noteworthy that we find no relaxation of the conformation to the negative ϕ region (α_R) as a result of the serine-to-glycine substitution (Table 4), showing either that hydrogen bonding by the hydroxyl group is not required for maintaining this unfavorable backbone conformation or, more likely, that this conformation is required to position the side chain and CO group within the binding site. Approximately 1 Å from the absent Ser130 OH group we see a single oxygen atom of a CH_2SO_3 fragment of a disordered HEPES molecule. The oxygen atom is equidistant (3.1 Å) from the ammonium groups of Lys73 and Lys234. The loss of the WT hydrogen bonds from Ser130 to Lys234 and to Ser70 increases the $C_\alpha-C_\alpha$ distance between Ser130 and Ser70 by 0.6 Å. Discussed below is an important consequence of this local expansion of the binding site, the loss of the catalytic water molecule found in all class A β-lactamases between Ser70, Glu166, and Asn170 (Figure 5). In this apo Ser130Gly variant, however, significant electron density at the expected

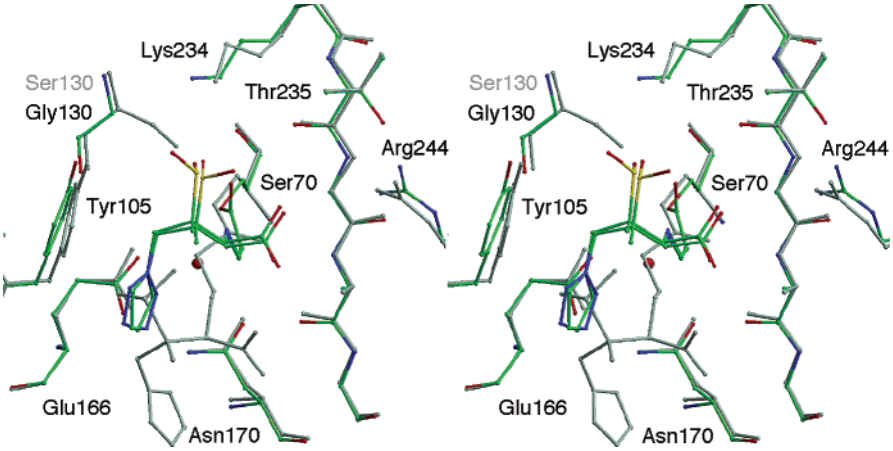

FIGURE 4: Overlay of the acyclic tazobactam intermediates in Ser130Gly (green) and WT (gray) SHV-1 (*17*) complexes. The acrylic acid adduct on Ser130 of the WT complex is omitted for clarity, as is minor aldehyde **10** of the Ser130Gly complex. Only the catalytic water molecule is shown (red sphere).

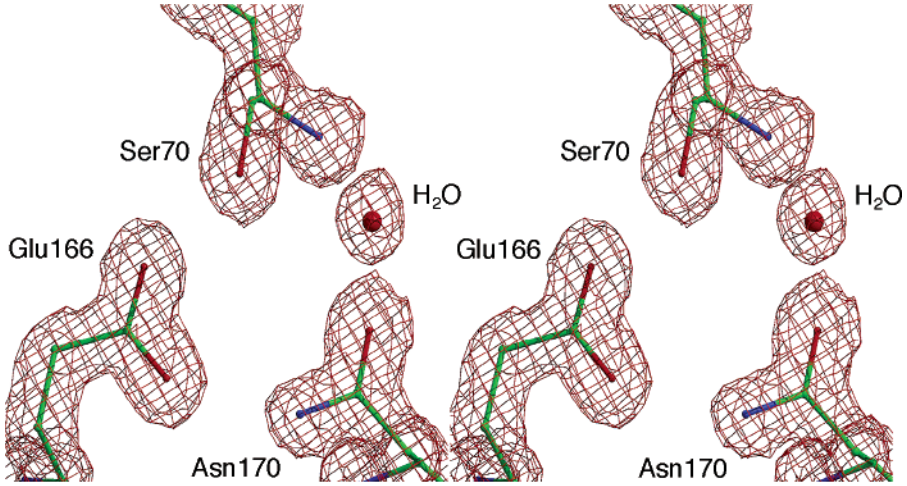

FIGURE 5: Stereoview of the $2F_o - F_c$ electron density in the uncomplexed Ser130Gly β-lactamase (contour level of 1.2σ). The "catalytic" water molecule normally found between Ser70, Glu166, and Asn170 in class A β-lactamases is absent. The water molecule in the oxyanion hole is at the right.

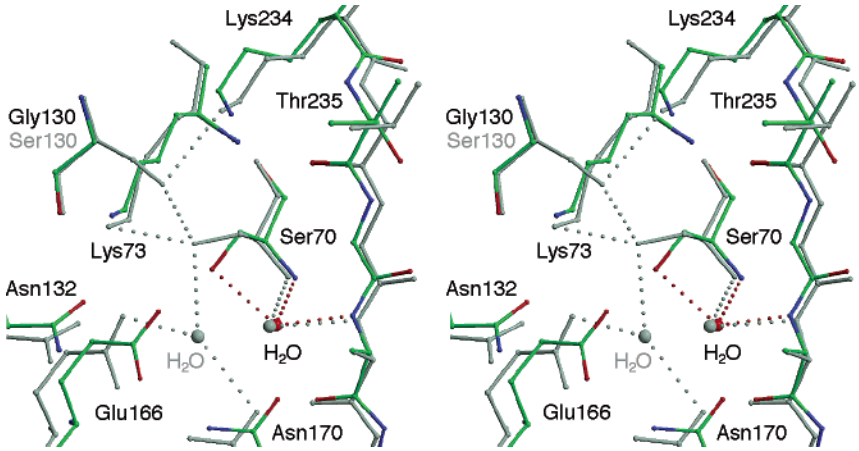

FIGURE 6: Comparison of catalytic sites in uncomplexed Ser130Gly (green) and WT (gray) SHV-1 (*22*) showing rotation and alteration in hydrogen bonding by the reactive Ser70. The catalytic water molecule in the WT structure (only) is at the left, and the water molecule in the oxyanion hole of both structures is at the right.

water position, i.e., within hydrogen bonding distance of all three residues, was not seen in electron density maps at any stage of the structure determination.

DISCUSSION

Before examining the reaction of tazobactam with the resistant Ser130Gly SHV-1 variant, we will discuss the unusual active site features of the uncomplexed (apo) variant. Generally, in class A β-lactamases, the hydroxyl group of Ser130 is hydrogen bonded to the side chains of Ser70 and Lys234 and its CO group is often bonded to Lys73. All four of these residues are absolutely conserved. Structurally, the Ser130−Ser70 hydrogen bond helps position the Ser70 side chain for catalysis, and the Ser130−Lys234 hydrogen bond connects the two main domains of the enzyme. Replacement of Ser130 with glycine is known to reduce the thermal stability of at least one β-lactamase (*13*). We have found that loss of the Ser130 linkages can also trigger a highly significant change in the binding site, the departure of the "catalytic" water molecule normally hydrogen bonded between Ser70, Glu166, and Asn170. This dehydration follows a rotation of the Ser70 hydroxyl group and the breaking of its strong hydrogen bond with Lys73 (from 2.8 to 3.5 Å) as well as with the catalytic water molecule (Figure 6). Ser70 now hydrogen bonds to another water molecule in the oxyanion hole (2.8 Å). The release of the catalytic water molecule is accompanied by 0.75 Å shifts of Glu166 and Asn170 relative to their positions in WT. [We note that the displacement of this strongly hydrogen bonded water molecule had been predicted in this particular variant by simulated annealing calculations (*12*).] While a role for Ser130 in catalysis has been debated for more than a decade (*4*, *15*, *16*), it can now be firmly concluded that in the precatalytic state Ser130 is clearly required for orienting the reactive side chain of Ser70 and ensuring the hydrogen bonding of Ser70 to both Lys73 and the catalytic water molecule.

Catalytic Mechanism. The absence of the Glu166-activated water molecule in the catalytic site of the apo variant, and the elimination of the signature hydrogen bond between Ser70 and Lys73, together raise the question about how the reactive Ser70 in this variant is deprotonated prior to acylation by β-lactam substrates or substrate-like inhibitors. It is known that this Ser130Gly variant is active on β-lactam substrates and inhibitors (*12*), albeit weakly, and we show here that it is acylated by an inhibitor such as tazobactam. How can this acylation happen, given either of two proposed mechanisms for abstracting the proton from Ser70, one using

the Glu166-activated water molecule (*31*, *32*) and the other using a neutral Lys73 hydrogen bonded to Ser70 (*15*)? Somehow, deprotonation of Ser70 occurs during binding of tazobactam to the variant, and the resulting seryl complex now contains a water molecule in the expected location among Ser70, Glu166, and Asn170. It is conceivable that entry of the inhibitor's β-lactam carbonyl group into the oxyanion hole will displace the water molecule residing there, forcing the hydroxyl group of Ser70 to rotate away and reform its normal hydrogen bonds with Lys73 and with a newly arrived catalytic water molecule.

Inhibition Mechanism. A reaction scheme for the irreversible inhibition of a WT β-lactamase (Figure 1) shows the pathways open to a variant lacking Ser130. Species **2**, formed by the acylation of the reactive Ser70, converts to acyclic tautomers (**3**−**5**) with ring opening and departure of the sulfinic group. The imine **3** and enamine tautomers **4** and **5** can undergo normal catalytic hydrolysis at the Ser70 ester linkage by the Glu166-activated water molecule conserved in all crystal structures of class A β-lactamases (*4*). This normal deacylation at Ser70 is the primary hydrolysis reaction, and it produces product **6** and a regenerated Ser70. In addition, however, a two-step hydrolysis of the reactive imine **3** can occur, first at C5 to produce aldehydes **10** and **11** and then at Ser70 to regenerate the active enzyme. Importantly, in the WT SHV-1 β-lactamase, a small fraction (*12*) of tazobactam molecules follows another path in which imine **3** undergoes a nucleophilic attack at C5 by the hydroxyl group of Ser130, which produces a bridging species **8**. Hydrolysis at Ser70 leads to the rather stable vinyl carboxylic acid adduct on Ser130, confirmed by X-ray crystallography (*17*). The structure showed that this Ser130 adduct is well anchored in the binding site so that it prevents entry of another inhibitor (or β-lactam substrate) molecule and effectively results in an irreversible inactivation of the WT β-lactamase.

Resistance by the Variant Enzyme. In the Ser130Gly variant, a good nucleophile is now unavailable for coupling with reactive intermediate **3**, though we see a water molecule near the position of the absent Ser130 OH group. Without the steric presence of the serine side chain, the linear **3**−**4** tazobactam species has more freedom of movement and, unlike the intermediate in the WT enzyme (*17*), has pulled out of the oxyanion hole. This out-of-hole species will be very resistant to catalytic hydrolysis at Ser70 by the Glu166-activated water molecule because the carbon atom of the ester carbonyl group is now quite distant (3.7 Å) and poorly positioned. The intermediate is vulnerable to attack at C5 by other water molecules. The resulting aldehyde **10** is found with its ester carbonyl group in the oxyanion hole, primed for normal hydrolysis at Ser70 by the activated water molecule. Without Ser130, then, the variant obviously avoids being irreversibly labeled by tazobactam at Ser130, but it can be transiently inhibited during a less efficient multistep hydrolysis.

CONCLUSION

We have described the structure of a class A β-lactamase lacking the strictly conserved Ser130, in both complexed and apo forms. The hydroxyl group of this serine is said to have both structural and possibly catalytic roles (*13*−*15*), and it is a well-placed nucleophile exploited by important mechanism-based inhibitors (*21*) such as clavulanic acid (*18*) and tazobactam (*17*, *19*, *20*). Spontaneous mutation of Ser130 is rarely found in clinical isolates and is documented in only a single SHV variant of 54 variants and in three TEM variants of 133 (see www.lahey.org/studies/webt.asp). These few Ser130 variants, always substituted with glycine, have so far arisen only in response to the use of mechanism-based inhibitors, not to third-generation β-lactam substrates such as cefotaxime or ceftazidime. Not surprisingly, the inhibitor-resistant variants are poorer catalysts for the turnover of most β-lactam substrates, yet they adequately provide for the survival of the pathogen.

Strangely, in the Ser130Gly apo crystal structure, the Glu166-activated water molecule, believed to be used for deprotonating the reactive Ser70 (*4*, *32*), and for hydrolysis of the acyl intermediate, is not observed in the electron density map, yet it is seen in the crystal structure of the tazobactam complex. Clearly, at an initial stage of the binding or reaction, the inhibitor induces or stabilizes an enzyme conformation which is able to fix the needed water molecule among Ser70, Glu166, and Asn170. Therefore, despite a 60-fold weaker binding with tazobactam (*12*), probably due to the loss of a Ser130 hydrogen bond to the C3 carboxylic acid group of the inhibitor (*14*), the variant class A β-lactamase becomes rehydrated and reconfigured for acylation at Ser70. The complexed crystal structure indicates that subsequent deacylation of the Ser70-bound intermediate will be severely hindered, but not prevented, because of the inhibitor's misalignment for oxyanion stabilization.

ACKNOWLEDGMENT

X-ray data were collected at the Institute of Materials Science of The University of Connecticut. We thank Dr. Michiyoshi Nukaga for assistance and helpful discussions.

REFERENCES

1. Pratt, R. F. (1992) in *The Chemistry of β-Lactams* (Page, M. I., Ed.) pp 229−271, Blackie Academic & Professional, London.
2. Bush, K., and Mobashery, S. (1998) in *Resolving the Antibiotic Paradox* (Rosen, B., and Mobashery, S., Eds.) pp 71−98, Kluwer Academic/Plenum, New York.
3. Sandanayaka, V. P., and Prashad, A. S. (2002) Resistance to β-lactam antibiotics: Structure and mechanism-based design of β-lactamase inhibitors, *Curr. Med. Chem. 9*, 1145−1165.
4. Matagne, A., Lamotte-Brasseur, J., and Frere, J.-M. (1998) Catalytic properties of class A β-lactamases: efficiency and diversity, *Biochem. J. 330*, 581−598.
5. Bush, K. (2001) New β-lactamases in Gram-negative bacteria: Diversity and impact on the selection of antimicrobial therapy, *Clin. Infect. Dis. 32*, 1085−1089.
6. Zhang, Z., Yu, Y., Musser, J. M., and Palzkill, T. (2001) Amino acid sequence determinants of extended spectrum cephalosporin hydrolysis by the class C P99 β-lactamase, *J. Biol. Chem. 276*, 46568−46574.
7. Yang, Y., Rasmussen, B. A., and Shlaes, D. M. (1999) Class A β-lactamases: enzyme−inhibitor interactions and resistance, *Pharmacol. Ther. 83*, 141−151.
8. Chaibi, E. B., Sirot, D., Paul, G., and Labia, R. (1999) Inhibitor-resistant TEM β-lactamases: phenotypic, genetic and biochemical characteristics, *J. Antimicrob. Chemother. 43*, 447−458.
9. Knox, J. R. (1995) Extended-spectrum and inhibitor-resistant TEM-type β-lactamases: mutations, specificity, and three-dimensional structure, *Antimicrob. Agents Chemother. 39*, 2593−2601.
10. Lin, S., Thomas, M., Shlaes, D. M., Rudin, S. D., Knox, J. R., Anderson, V., and Bonomo, R. A. (1998) Kinetic analysis of an inhibitor-resistant variant of the OHIO-1 β-lactamase, an SHV-family class A enzyme, *Biochem. J. 333*, 395−400.

11. Bermudes, H., Jude, F., Chaibi, E. B., Arpin, C., Bebear, C., Labia, R., and Quentin, C. (1999) Molecular characterization of TEM-59 (IRT-17), a novel inhibitor-resistant TEM-derived β-lactamase in a clinical isolate of *Klebsiella oxytoca*, *Antimicrob. Agents Chemother. 43*, 1657−1661.
12. Helfand, M. S., Bethel, C. R., Hujer, A. M., Hujer, D. M., Anderson, V. E., and Bonomo, R. A. (2003) Understanding resistance to β-lactams and β-lactamase inhibitors in the SHV β-lactamase, *J. Biol. Chem. 278*, 52724−52729.
13. Jacob, F., Joris, B., Lepage, S., Dusart, J., and Frere, J.-M. (1990) Role of the conserved amino acids of the "SDN" loop in a class A β-lactamase studied by site-directed mutagenesis, *Biochem. J. 271*, 399−406.
14. Juteau, J.-M., Billings, E. M., Knox, J. R., and Levesque, R. C. (1992) Site-saturation mutagenesis and three-dimensional modelling of ROB-1 define a substrate binding role of Ser130 in class A β-lactamases, *Protein Eng. 5*, 693−701.
15. Strynadka, N. C. J., Adachi, H., Jensen, S. E., Johns, K., Sielecki, A., Betzel, C., Sutoh, K., and James, M. N. G. (1992) Molecular structure of the acyl-enzyme intermediate in β-lactam hydrolysis at 1.7 Å resolution, *Nature 359*, 700−705.
16. Ishiguro, M., and Imajo, S. (1996) Modeling study on a hydrolytic mechanism of class A β-lactamases, *J. Med. Chem. 39*, 2207−2218.
17. Kuzin, A. P., Nukaga, M., Nukaga, Y., Hujer, A. M., Bonomo, R. A., and Knox, J. R. (2001) Inhibition of the SHV-1 β-lactamase by sulfones: Crystallographic observation of two reaction intermediates with tazobactam, *Biochemistry 40*, 1861−1866.
18. Brown, R. P. A., Aplin, R. T., and Schofield, C. J. (1996) Inhibition of TEM-2 β-lactamase from *Escherichia coli* by clavulanic acid: observation of intermediates by electrospray ionization mass spectrometry, *Biochemistry 35*, 12421−12432.
19. Yang, Y., Janota, K., Tabei, K., Huang, N., Siegel, M. M., Lin, Y.-I., Rasmussen, B. A., and Shlaes, D. M. (2000) Mechanism of inhibition of the class A β-lactamases PC1 and TEM-1 by tazobactam: observation of reaction products by electrospray ionization mass spectrometry, *J. Biol. Chem. 275*, 26674−26682.
20. Pagan-Rodriguez, D., Zhou, X., Simmons, R., Bethel, C. R., Hujer, A. M., Helfand, M. S., Jin, Z., Guo, B., Anderson, V. E., Ng, L. M., and Bonomo, R. A. (2004) Tazobactam inactivation of SHV-1 and the inhibitor-resistant Ser130-Gly SHV-1 β-lactamase, *J. Biol. Chem. 279*, 19494−19501.
21. Imtiaz, U., Billings, E. M., Knox, J. R., Manavathu, E. K., Lerner, S. A., and Mobashery, S. (1993) Inactivation of class A β-lactamases by clavulanic acid: The role of arginine-244 in a nonconcerted sequence of events, *J. Am. Chem. Soc. 115*, 4435−4442.
22. Kuzin, A. P., Nukaga, M., Nukaga, Y., Hujer, A. M., Bonomo, R. A., and Knox, J. R. (1999) Structure of the SHV-1 β-lactamase, *Biochemistry 38*, 5720−5727.
23. Hujer, A. M., Hujer, K. M., and Bonomo, R. A. (2001) Mutagenesis of amino acid residues in the SHV-1 β-lactamase: the premier role of Gly238Ser in penicillin and cephalosporin resistance, *Biochim. Biophys. Acta 1547*, 37−50.
24. Kissinger, C. R. (1999) Rapid automated molecular replacement by evolutionary search, *Acta Crystallogr. D55*, 484−491.
25. Brunger, A. T., Adams, P. D., Clove, G. M., Delano, W. L., Gros, P., Grosse-Kunstleve, R. W., Jiang, J.-S., Kuszewski, J., Nilges, M., Pannu, N. S., Read, R. J., Rice, L. M., Simonson, T., and Warren, G. L. (1998) CNS (Crystallography and NMR System), *Acta Crystallogr. D54*, 905−921.
26. Sack, J. S., and Quiocho, F. A. (1997) CHAIN: A crystallographic modeling program, *Methods Enzymol. 277*, 158−173.
27. Maveyraud, L., Mourey, L., Kotra, L. P., Pedelacq, J.-D., Guillet, V., Mobashery, S., and Samama, J.-P. (1998) Structural basis for clinical longevity of carbapenem antibiotics in the face of challenge by the common class A β-lactamases from the antibiotic-resistant bacteria, *J. Am. Chem. Soc. 120*, 9748−9752.
28. Swaren, P., Massova, I., Bellettini, J. R., Bulychev, A., Maveyraud, L., Kotra, L. P., Miller, M. J., Mobashery, S., and Samama, J.-P. (1999) Elucidation of mechanism of inhibition and X-ray structure of the TEM-1 β-lactamase from *E. coli* inhibited by a N-sulfonyloxy-β-lactam, *J. Am. Chem. Soc. 121*, 5353−5359.
29. Beadle, B. M., Trehan, I., and Shoichet, B. K. (2002) Structural milestones in the reaction pathway of an amide hydrolase: substrate, acyl, and product complexes of cephalothin with AmpC β-lactamase, *Structure 10*, 413−424.
30. Padayatti, P. S., Helfand, M. S., Totir, M. A., Carey, M. P., Hujer, A. M., Carey, P. R., Bonomo, R. A., and van den Akker, F. (2004) Tazobactam forms a stoichiometric *trans*-enamine intermediate in the E166A variant of SHV-1 β-lactamase: 1.63 Å crystal structure, *Biochemistry 43*, 843−848.
31. Minasov, G., Wang, X., and Shoichet, B. K. (2002) An ultrahigh-resolution structure of TEM-1 β-lactamase suggests a role for Glu166 as the general base in acylation, *J. Am. Chem. Soc. 124*, 5333−5340.
32. Nukaga, M., Mayama, K., Hujer, A. M., Bonomo, R. A., and Knox, J. R. (2003) Ultrahigh-resolution structure of a class A β-lactamase: On the mechanism and specificity of the extended-spectrum SHV-2 enzyme, *J. Mol. Biol. 328*, 289−301.
33. McRee, D. E. (1999) XtalView/Xfit: A versatile program for manipulating atomic coordinates and electron density, *J. Struct. Biol. 125*, 156−165.
34. Merritt, E. A., and Bacon, D. J. (1997) Raster3D: Photo-realistic molecular graphics, *Methods Enzymol. 277*, 505−524.
35. Kraulis, P. (1991) MOLSCRIPT: a program to produce both detailed and schematic plots of protein structures, *J. Appl. Crystallogr. 24*, 946−950.

BI0487903